SMALL-SCALE CHARACTERISTICS OF THE FLUCTUATING PASSIVE SCALAR FIELD IN A TURBULENT BOUNDARY LAYER

L.P. Dasi & D.R. Webster
School of Civil & Environmental Engineering
Georgia Institute of Technology, Atlanta, Georgia 30332, USA
lakshmi.dasi@ce.gatech.edu, dwebster@ce.gatech.edu

ABSTRACT

The objective is to study the effects of mean scalar gradient on the structure functions and power spectrum of the fluctuating scalar field. The scalar field is created by a continuous iso-kinetic release of a passive scalar ($Sc \approx 1000$) in a turbulent boundary layer at mid-depth of an open channel flow ($Re = 1\times10^4$). Measurements of the scalar field are performed using the planar laser induced fluorescence (PLIF) technique at four distances downstream of the source in a vertical plane through the plume centerline. Scaling exponents in the inertial-convective range, estimated from the second and higher (even) order structure functions, show dependence on the longitudinal scalar gradient. As the mean longitudinal scalar gradient increases, the longitudinal exponents decrease from the isotropic expectation of $n/3$. Scaling behavior is also noted in the viscous-convective range of the variance spectrum. The exponent for the dependence on the wavenumber increases in proportion to the logarithm of the mean longitudinal scalar gradient. Overall, the scaling behavior appears to be dependent on the mean field and agrees with isotropic expectations as the mean scalar gradient tends toward zero.

INTRODUCTION

Mixing of passive scalars in turbulent flows has tremendous significance in both applied and theoretical research. For instance, researchers in recent years have addressed scalar mixing in the context of pollutant impact in the atmosphere and ocean, chemical mixing, and fundamental small-scale behavior. The promise of a universal characterization of the fluctuating passive scalar field at a local scale has motivated many experimental and theoretical studies with varying degrees of success (Sreenivasan and Antonia, 1997).

The most common mathematical tools used to describe the local structure of fluctuating scalar fields are structure functions and the variance spectrum as a function of wavenumber. The n^{th} order structure function for the passive scalar field is defined by:

$$\left\langle \Delta\theta_r^n \right\rangle = \left\langle \left(\theta(\boldsymbol{x}+\boldsymbol{r}) - \theta(\boldsymbol{x})\right)^n \right\rangle \qquad (1)$$

where n is the order of the function, θ is the fluctuation of the scalar from the mean, $\boldsymbol{r}$ is the separation vector, and $\langle\ \rangle$ denotes ensemble averaging. The structure function is called longitudinal when $\boldsymbol{r}$ is in the direction of the mean flow and transverse when $\boldsymbol{r}$ is orthogonal to the mean flow. The basic question for on-going research is: *Does the behavior of the structure functions and variance spectrum possess universal characteristics (i.e. independent of flow boundary conditions)*?

Kolmogorov's local isotropy phenomenology of the fluctuating velocity field first addressed the question of universality through dimensional arguments and the concept of self-similar eddies that transfer energy to the dissipative scales via the energy cascade (Kolmogorov, 1941). Analogous theoretical arguments were subsequently developed for passive scalars by Obukhov (1949), Corrsin (1951), and Batchelor (1959). The theory proposed an analogy of the inertial range for the passive scalar statistics for large Peclet number. When the velocity field has an inertial range, several scaling regimes may exist for the high Schmidt number passive scalar variance spectrum and structure functions. The inertial-convective range is defined as the range with negligible effects of viscosity and diffusivity (for the

wavenumber interval $\frac{1}{L} << k << \frac{1}{\eta}$, where L is the integral length scale). The viscous-convective range is defined as the range where viscous effects start to play a role, while molecular diffusivity does not ($\frac{1}{\eta} << k << \frac{1}{\eta_B}$). The viscous-diffusive range is defined for the very high wavenumbers corresponding to length scales of the order of the Batchelor scale ($k \approx \frac{1}{\eta_B}$).

The phenomenology model for passive scalars, named KOC theory (Kolmogorov-Obukhov-Corrsin), provided the scaling behavior of the scalar structure functions and variance spectrum (which were assumed to be independent of the direction of r and k). According to this phenomenology theory for the regimes described above, the structure functions and variance spectrum follow a simple scaling behavior given by:

$$\left\langle \Delta\theta_r^n \right\rangle \propto r^{\zeta^n} \tag{3}$$

$$E(k) \propto k^{\mu} \tag{4}$$

The classic theory predicts ζ^n to be equal to $n/3$ and μ to be $-5/3$ in the interial-convective range. The phenomenological model failed to fully capture the characteristics of the local structure of the passive scalar field. In particular, the scaling exponents for higher order structure functions were smaller than $n/3$ and appeared to reach a constant for large n (now referred as saturation of the scaling exponents). The failure was attributed to the fact that KOC did not account for the intermittency of the dissipation of the scalar variance (Obukhov, 1962). The refined similarity hypotheses for passive scalars (RSHP) incorporated the intermittency to yield better agreement between theory and experimental observation for the scaling exponents (Monin and Yaglom, 1975). Although the scaling exponents predicted by RSHP were not universal, the predictions assumed some of the characteristics of the dissipation field to be universal (such as a joint log-normal distribution between the fluctuating dissipation rates of kinetic energy and scalar variance). Nevertheless, the validity of RSHP (with its assumption of local isotropy) is questionable due to the fundamentally anisotropic nature of the scalar field (Shraiman and Siggia, 2000). Accepting the fact that the scalar field is anisotropic, a fundamental question is: *How does the scaling behavior of the structure functions, or in general any local characteristic, relate to global characteristics (i.e. mean scalar field)*?

The objective of this study is to examine the effects of the large-scale scalar gradient on scaling behavior of the structure functions for a high Schmidt number passive scalar. This will be achieved by studying the effect of varying mean concentration gradient on the small-scale characteristics as described by the structure functions and variance spectrum for the various scaling regimes.

EXPERIMENTAL PROCEDURE

Experiments are conducted to measure the fluctuating scalar field in an equilibrium turbulent boundary layer. Measurements are performed in a 1.07 m wide, 24.4 m long tilting flume for fully developed, uniform flow conditions ($Re = 1\times10^4$ based on mean velocity of 100 mm/s and water depth of 100 mm). The passive scalar field is generated by a leaky source (nozzle of diameter 4.7 mm) of the laser fluorescent dye Rhodamine 6G ($Sc \approx 1000$) placed along the flume centerline at 50 mm from the flume bed (Fig. 1). The Kolmogorov length scale, $\eta \sim (\nu^3/\varepsilon)^{1/4}$, and the Batchelor length scale, $\eta_B \sim (\nu\kappa^2/\varepsilon)^{1/4}$, for this flow and plume are estimated to be 0.7 mm and 20 μm, respectively. A coordinate system is defined by the longitudinal coordinate, x, and vertical coordinate, y, with the origin at the nozzle location.

The planar laser-induced fluorescence (PLIF) technique is used to measure time records of the scalar field in a vertical plane parallel to the flow direction on the centerline of the plume. The laser sheet (created by sweeping the laser beam with a scanning mirror) causes the dye to fluoresce and an 8-bit digital CCD camera (1008×1018 pixels) captures the emitted light over a 20 mm × 20 mm region (thus, the image resolution is 20 μm/pixel). The laser beam passes through a beam expander and convex lens (1 m focal length), to give a $1/e^2$ diameter of 20 μm. Thus, the measurement technique resolves the Batchelor length scale in all three directions. The data is captured at 25 Hz with a total of 32,512 samples. Due to finite disk capacity, a subset of the images (either 6×1018 or 1008×6 pixels) located symmetrically about the nozzle centerline was saved in real time to the hard drive for further data analysis. The laser beam sweeps through the flow very rapidly, essentially freezing the flow structure (less than 1% error due to advection of the flow structure). A careful calibration of the relationship of light intensity to the dye concentration is performed *in situ*.

In order to study the variation of small-scale characteristics with respect to mean scalar gradient, measurements are performed at four longitudinal distances from the point source: 250 mm, 500 mm, 1 m, and 2 m. The uniform release conditions and equilibrium boundary layer yield a constant mean velocity gradient among the measurements, while the mean concentration gradient varies over a couple orders of magnitude.

RESULTS AND DISCUSSION

Figure 2 shows a sample of the measured instantaneous scalar field, $\Theta(x,y)$, normalized by the source concentration, Θ_0. The normalization is implied for the remainder of this paper. It is evident from the figure that the scalar field is highly intermittent in space and time and takes zero value over most of the region. In contrast, a high momentum release would produce a relatively homogeneous instantaneous field. In order to study the structure functions, the scalar field is decomposed using the Reynolds decomposition: $\Theta = \langle\Theta\rangle + \theta$ where $\langle\ \rangle$ denotes time average.

Figure 3 shows the centerline variation of the mean scalar concentration and suggests a power law decay over the last three measurement locations. The first data point does not follow the power law due to the relative diffusion phenomena that occurs when the mean size of scalar concentration filaments is smaller than the eddy size corresponding to the integral length scale. The concentration gradient in the x-direction is shown in Table 1.

Table 1: Concentration gradient in x-direction

x (m)	$d\langle\Theta\rangle/dx$ (m^{-1})
0.25	-7.1×10^{-2}
0.5	-3.6×10^{-3}
1.0	-9.0×10^{-4}
2.0	-2.2×10^{-4}

Figure 4 shows the second order structure functions in the longitudinal and transverse directions at four distances downstream. The separation distance, r, is normalized by the Batchelor length scale, η_B. An inertial-convective range scaling is evident in the structure functions.

Figure 5 shows the estimated inertial-convective range scaling exponents, ζ_x^n and ζ_y^n, for the structure functions of order 2, 4, 6, 8, and 10 as a function of the longitudinal location. It is clear that longitudinal and transverse scaling exponents do not agree, thus indicating anisotropic conditions. The longitudinal scaling exponents increase with x, while the transverse exponents decrease with x.

A different perspective of this trend is achieved by plotting the scaling exponents as a function of the mean scalar gradient (Fig. 6). Figure 6(a) reveals the dependence of the longitudinal inertial-convective range exponents with respect to the magnitude of the mean scalar gradient. As the mean scalar gradient increases the longitudinal exponents decrease for the higher order structure functions. In contrast, the exponent for the second order structure function is nearly constant. For small values of the scalar gradient, the exponents agree well with the $n/3$ prediction, while the exponents appear to be saturated for higher values of mean scalar gradient. It may be conjectured that as the mean gradient tends to zero, the exponents tend to the respective isotropic expectation of $n/3$.

Figure 6(b) shows the dependence of the inertial-convective range exponents for the transverse structure functions on the mean longitudinal scalar gradient. The exponents appear to increase in proportion to the logarithm of the scalar gradient at larger values of the gradient. It must be noted that this trend is perhaps due to the evolving magnitude of the mean vertical scalar gradient. Hence, we leave this point for a future discussion relative to the mean vertical gradient.

Figure 7 shows the saturation of the longitudinal scaling exponents under the influence of varying mean scalar gradients. From the figure it is evident that the exponents agree with the isotropy expectation far from the source where the mean gradient magnitude is small (Fig. 7a). The variation with n saturates for a moderate mean gradient and asymptotes to near $\ln\left(n^{1/2}\right)$ behavior for higher values of the mean longitudinal gradient (Fig. 7b). The data corresponding to the two largest mean scalar gradients agree well with data complied by Warhaft (2000). A more theoretical justification for this behavior is necessary and will be addressed in the future. Figure 8 shows similar saturation behavior for the transverse inertial-convective range scaling exponents and suggests that the vertical gradient may have an important influence on the behavior of the transverse structure functions.

Figure 9 shows the scalar variance spectrum with respect to both longitudinal and transverse wavenumbers, k_x and k_y. As suggested from the second order structure functions, there is an inertial-convective range where the slope is close to the isotropy expectation of $-5/3$. More interestingly, the viscous-convective range appears to have a scaling behavior. Figure 10 shows the scaling exponents of the variance spectra in the viscous-convective range as a function of mean longitudinal scalar gradient. The exponents μ_x and μ_y appear to decrease with increasing mean longitudinal gradient, thus the spectrum in the viscous-convective range falls off at a steeper rate.

CONCLUSION

The effect of the mean scalar gradient on the small scale characteristics of the fluctuating scalar field is examined. Visualization suggests highly intermittent dynamics of the scalar field. The structure functions in the longitudinal and transverse directions reveal anisotropic behavior. Small-scale characteristics such as the scaling exponents of the structure functions of orders 2, 4, 6, 8, and 10 for the inertial-convective

range depend on the mean scalar gradient. For small values of the longitudinal scalar gradient the scaling exponents of the longitudinal structure functions appear to agree with the isotropic expectation of $n/3$. The exponents saturate for moderate mean gradient and asymptote to $\ln\left(n^{1/2}\right)$ behavior for larger mean gradient. The exponents of the transverse structure function also appear to vary, but the observed trend may be related with the vertical mean scalar gradient, which was not quantified by the current measurements. The variance spectra reveal the dependence of viscous-convective range scaling behavior with respect to mean scalar gradient. The exponents for the dependence on the longitudinal wavenumber in this range appear to decrease with increasing magnitude of the mean scalar gradient.

As a final remark, the local structure of the scalar fluctuations is indeed related to the mean scalar field. Most of the previous experiments on passive scalars have been with non-zero mean scalar gradient and therefore any deviation from isotropic expectations is no surprise. The preliminary data presented here indicate that further studies need to be conducted in order to strongly quantify the relationship between the local structure and the mean field.

REFERENCE

Batchelor, G.K., 1959, "Small-scale variation of convected quantities like temperature in turbulent fluid. Part 1. General discussion and the case of small conductivity," *J. Fluid Mech.*, Vol. 5, pp. 113-133.

Corrsin, S., 1951, "On the spectrum of isotropic temperature fluctuations in isotropic turbulence," *J. Applied Physics*, Vol. 22, pp. 469.

Kolmogorov, A.N., 1941, "The local structure of turbulence in incompressible viscous fluid for very large Reynolds numbers," *Dolk. Akad. Nauk SSSR*, Vol. 30, pp. 301.

Monin, A.S., and Yaglom, A.M, 1975, "Statistical fluid mechanics, mechanics of turbulence," *MIT Press.* Vol 2.

Obukhov A.M., 1949, "Structure of the temperature field in turbulent flows," *Izvestiya Akademii Nauk SSSR, Geogr. and Geophys. Ser.*, Vol. 13, pp. 58.

Obukhov, A.M., 1962, " Some specific features of atmospheric turbulence," *J. Fluid Mech.*, Vol. 13, pp. 77-81.

Shraiman, B.I., and Siggia, E.D., 2000, "Scalar turbulence," *Nature*, Vol. 405, pp. 639-646.

Sreenivasan, K.R., and Antonia, R.A., 1997, "The phenomenology of small-scale turbulence," *Annu. Rev. Fluid Mech.*, Vol. 29, pp. 435-472.

Warhaft, Z., 2000, "Passive scalars in turbulent flows," *Annu. Rev. Fluid Mech.*, Vol. 32, pp. 203-240.

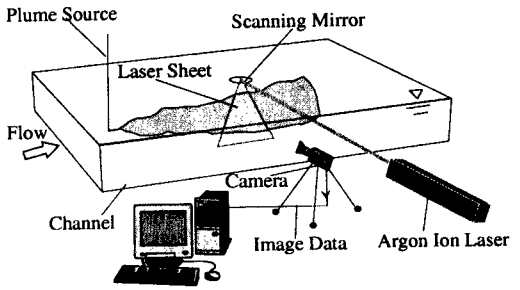

Figure 1 : Schematic of the experiment setup.

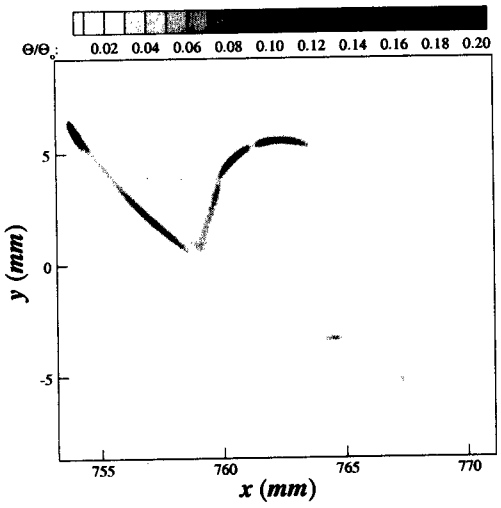

Figure 2 : Sample of the measured scalar field.

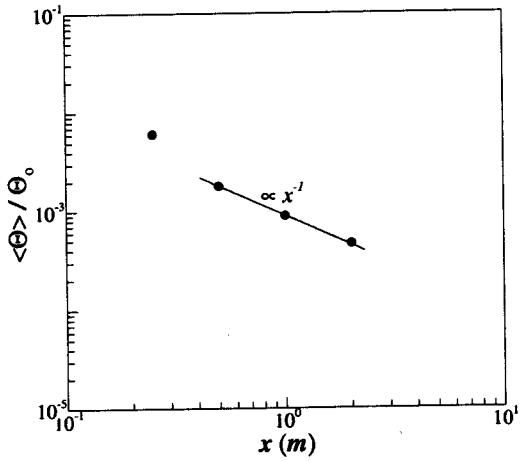

Figure 3 : Mean concentration along centerline of the plume.

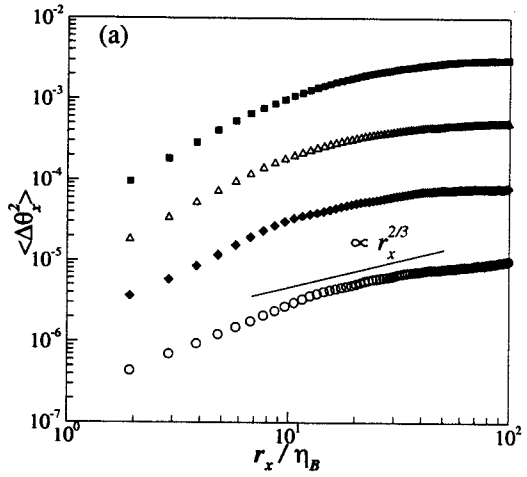

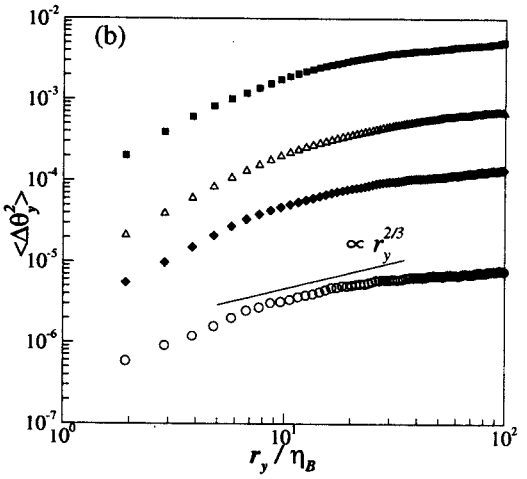

Figure 4 : Second order (a) longitudinal, and (b) transverse structure functions for x = 0.25 m (■), 0.5 m (Δ), 1 m (♦), and 2 m (○).

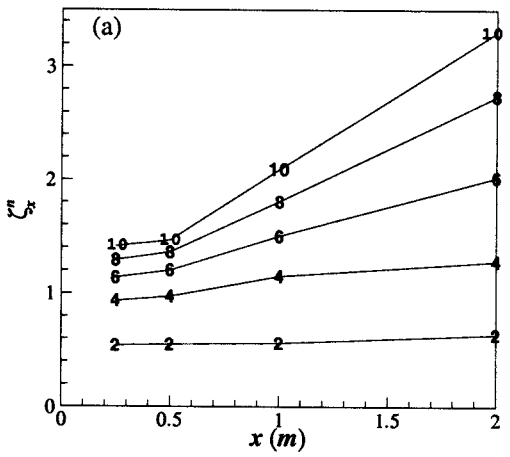

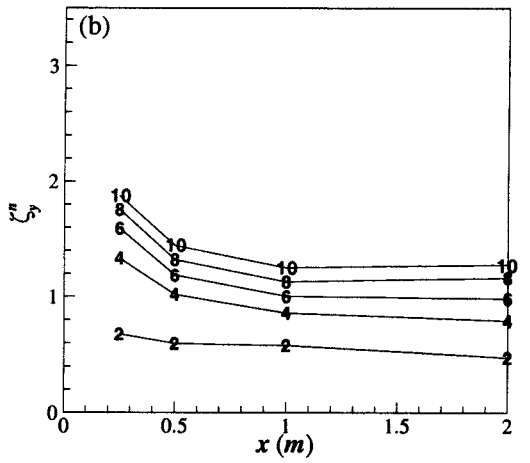

Figure 5 : Scaling exponents in the inertial-convective range of the (a) longitudinal, and (b) transverse structure functions. The symbol number corresponds to the order of the structure function.

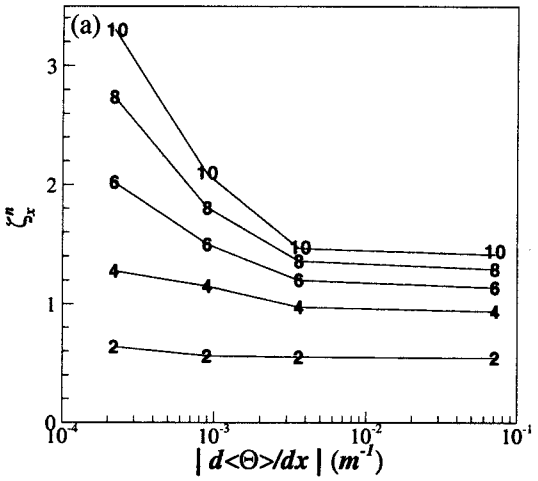

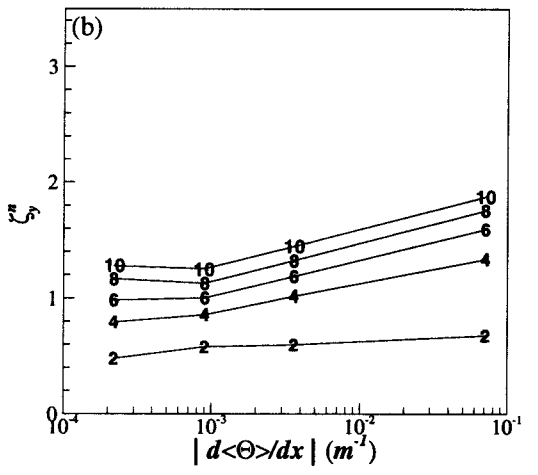

Figure 6 : Scaling exponents in the inertial-convective range of the (a) longitudinal, and (b) transverse structure functions as a function of mean scalar gradient magnitude. The symbol number corresponds to n .

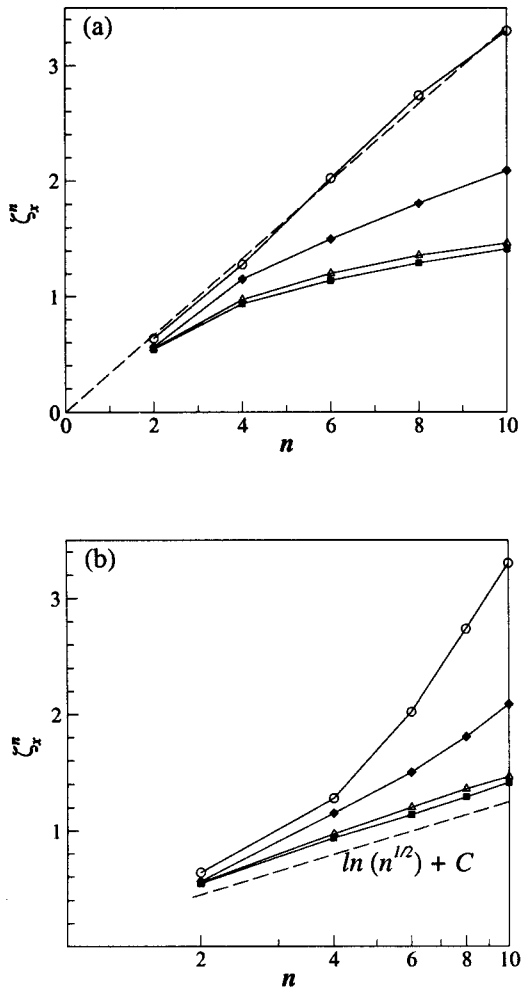

Figure 7 : Saturation of the longitudinal scaling exponents in the inertial-convective range on (a) linear, and (b) semi-log plots for x = 0.25 m (■), 0.5 m (Δ), 1 m (♦), and 2 m (○).

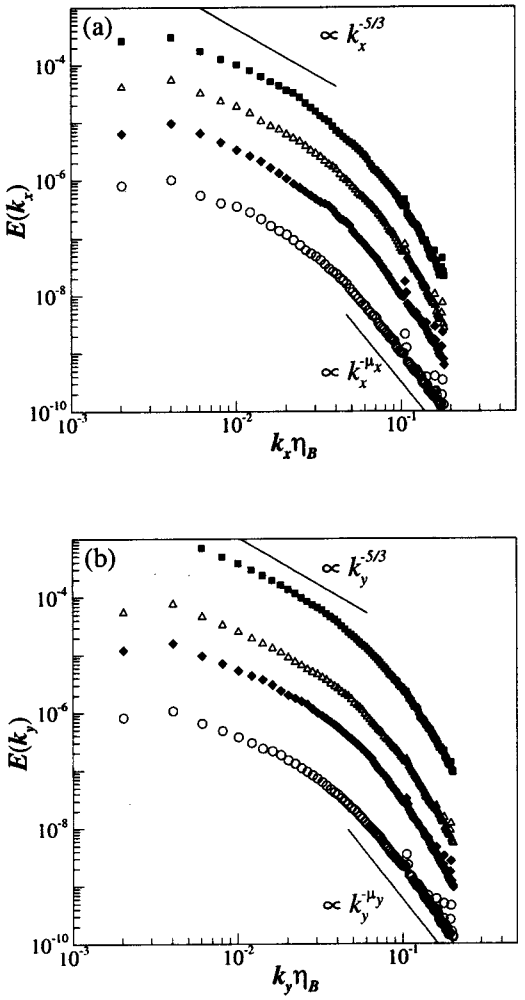

Figure 9 : Power spectra of the fluctuating scalar field along (a) longitudinal, and (b) transverse wavenumbers for x = 0.25 m (■), 0.5 m (Δ), 1 m (♦), and 2 m (○).

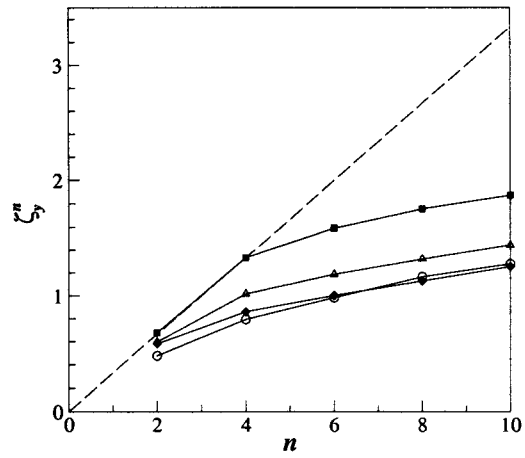

Figure 8 : Saturation of the transverse scaling exponents in the inertial-convective range for x = 0.25 m (■), 0.5 m (Δ), 1 m (♦), and 2 m (○).

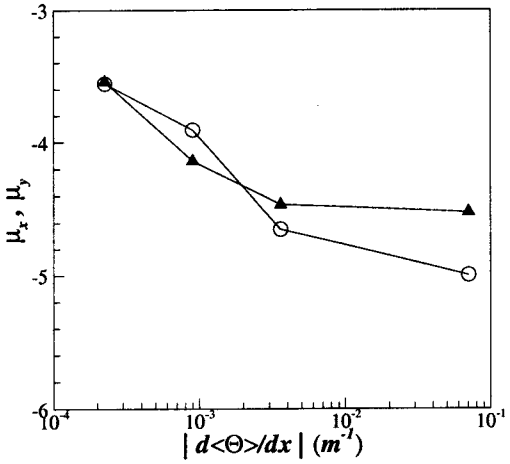

Figure 10 : Scaling exponent in the viscous-convective range for the longitudinal (O) and transverse (▲) scalar variance spectrum as a function of mean scalar gradient magnitude.